

Structural Characterization of Linear Three-Dimensional Random Chains: Energetic Behaviour and Anisotropy

David R. Avellaneda B.[1], Ramón E. R. González[2(✉)], Paola Ariza-Colpas[3], Roberto Cesar Morales-Ortega[3], and Carlos Andrés Collazos-Morales[4(✉)]

[1] Departamento de Estatística e Informática, Universidade Federal Rural de Pernambuco, Recife, Pernambuco CEP 52171-900, Brazil
[2] Departamento de Física, Universidade Federal Rural de Pernambuco, Recife, Pernambuco CEP 52171-900, Brazil
ramon.ramayo@ufrpe.br
[3] Departamento de Ciencias de la Computación y Electrónica, Universidad de la Costa, Barranquilla, Colombia
[4] Vicerrectoria de Investigaciones, Universidad Manuela Beltrán, Bogotá, Colombia
carlos.collazos@docentes.umb.edu.co

Abstract. In this work, we will make an energetic and structural characterization of three-dimensional linear chains generated from a simple self-avoiding random walk process in a finite time, without boundary conditions, without the need to explore all possible configurations. From the analysis of the energy balance between the terms of interaction and bending (or correlation), it is shown that the chains, during their growth process, initially tend to form clusters, leading to an increase in their interaction and bending energies. Larger chains tend to "escape" from the cluster when they reach a number of "steps" $N >\sim 1040$, resulting in a decrease in their interaction energy, however, maintaining the same behavior as flexion energy or correlation. This behavior of the bending term in the energy allows distinguishing chains with the same interaction energy that present different structures. As a complement to the energy analysis, we carry out a study based on the moments of inertia of the chains and their radius of gyration. The results show that the formation of clusters separated by "tails" leads to a final "prolate" structure for this type of chain, the same structure evident in real polymeric linear chains in a good solvent.

Keywords: Self-avoiding random walk · Linear chains · Interaction energy · Bending energy · Moment of inertia · Radius of gyration · Asphericity · Prolate structure

1 Introduction

The self-excluding random walk (SAW) is a very simple and useful model for understanding some physical phenomena. Under certain conditions, SAWs can model some

© Springer Nature Switzerland AG 2021
O. Gervasi et al. (Eds.): ICCSA 2021, LNCS 12949, pp. 179–191, 2021.
https://doi.org/10.1007/978-3-030-86653-2_13

properties of real linear chains. SAW is not just a useful modeling tool; the field has advanced significantly in the last 50 years, its study has stimulated theoretical developments in areas such as mathematics, physics and computer science and is widely accepted as the main model for polymers diluted [1–4].

We use a model based on a self-excluding walk to generate an ensemble of three-dimensional linear chains. Our model does not consider all possible configurations of the system, avoiding high computational costs. It only considers a number of strings large enough to guarantee acceptable statistical confidence. The cubic network used does not have boundary conditions and the process is carried out in a "finite" time. In this article, we propose and study a conformational energy model based on the flexibility of linear chains that report realistic results and allows you to differentiate chains regardless of their structure. As part of the study, it was examined the balance between the energy of interaction between the "links" in the chain and the bending energy in order to find its relationship with the structure of the chains. This analysis is relevant because it allows differentiating between chains of equal interaction energy but with different structures.

The paper is organized as follows. In the next section, we speak briefly about the proposed algorithm, used to generate the linear chains. We also describe the energy models used, the calculation of the moment of inertia, and the asphericity, tools used for the characterization of the chains. The subsequent section is dedicated to the discussion of the results of our simulations and finally, we expose the conclusions of the work.

2 Methodology

2.1 Numerical Algorithm

The ensemble of linear chains was generated from the sequence of steps showed next, for a d − dimensional network, with free boundaries:

Step 1. Initially, the number of attempts $N^{'}$ is choosen. This variable will define the length of the chain.
Step 2. The origin of the coordinate system is choosen as the the origin of the chain.
Step 3. From the origin, the first step in the generation of the chain is choosen randomly, from the neighbourhood of the origin.
Step 4. The following steps are choosen, randomly, from the rest of the neighbourhood, excluding previously "visited" points. This step is the most important to ensure the SAW.
Step 5. Add the step to the walk (chain).
Step 6. When the number of new possible steps is zero or the number of attemps is reached, the process ends and the chain is saved.

For three-dimensional chains, $N < N^{'}$, this indicated that the "walker" usually gets stuck before the $N^{'}$ attempts.

2.2 Energy of Linear Chains

In our analysis, we use a definition of the interaction energy, which is based on the compactness of the chains [5–7]. We also examine the bending energy as a discrete

variable that characterizes the chain flexibility, as well as, its tangential correlations. The total energy of the chain is then, considered as the sum of the bending energy and the interaction energy.

Interaction Energy. Interaction energy accounts for the energy of the chain due to its compactness and it quantifies the short-range interactions (Von Neumann neighbourhood) for non-continuous monomers [5–7]. It reads as,

$$E = \sum_{i<j} e_{ij} \Delta\left(r_i - r_j\right). \tag{1}$$

where $\Delta(r_i - r_j) = 1$ if r_i and r_j are attached to the network, but i and j are not adjacent positions along the chain sequence and $\Delta(r_i - r_j) = 0$ for otherwise (see Fig. 1).

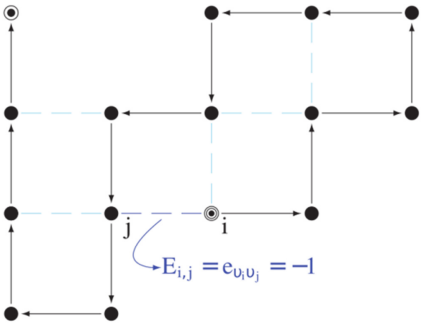

Fig. 1. 14-step 2d-chain that shows the values that the interaction takes Δ(ri - rj), where it adopts the values: 1, for the attachments but not adjacent sites (blue color) and 0 for the otherwise. (Color figure online)

The type of contact between the "links" determines the value of the factor e_{ij}. This variable, in turn, represents the potential energy of interaction between the "links" located in the position r_i and r_j respectively. For attractive "link-link" interaction, $e_{ij} = -1$.

Bending Energy. One of the basic characteristics of all macromolecules is their flexibility [8]. The polymer chains, in the pure state or in dissolution, may adopt different conformations depending on their flexibility. Chains with low flexibility will be more rigid and will tend, in the limit, to behave as a hard stick. On the other hand, when the flexibility is high, the chain may have large changes of direction within a few links. The flexibility of the polymer chain is related to the persistence length l_p. This can be defined as the average value of the maximum linear length of the chain configuration (it is also related to the Kuhn segment as $b = 2l_p$ [9]). For distances greater than l_p, the "memory" associated with the direction, up that point, adopted by the chain is lost. Thus, some energy is always required to fold the chains, which can happen up to at most the l_p. In our model, we use these properties of macromolecules in the definition of our bending energy term.

In the graph of Fig. 2, we show the correlation (in turn related to the flexibility) between u and u', two unit vectors that join three points of the chain (monomers h, i and j), and that

are separated by a distance l is given by [10]:

$$\langle \boldsymbol{u} \cdot \boldsymbol{u'} \rangle = \left[\left(1 - \left(b/l_p\right)\right)^{1/b} \right]^l \sim \exp\left(-l/l_p\right). \tag{2}$$

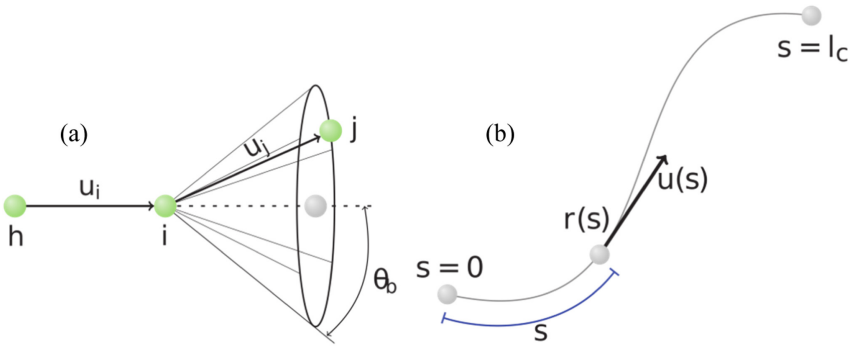

Fig. 2. Schematic representation of a section of the chain that shows high flexibility. Vectors of bond u_i with a fixed link angle between two consecutive monomers, (a). Chain conformation specifying $r(s)$ and the unit vector $u(s)$, (b).

At the limit, the conformation of the chain is a smooth curve as described in Fig. 2b. Using Eq. 2 it can be obtain the correlation function between $u(s)$ and $u(s^{'})$ of two segments of the chain, s and $s^{'}$, as a function of the persistence length l_p. This function shows that the directional correlation of two segments of a macromolecule, decreases exponentially with the growth of the chain length [8, 10, 11]:

$$c\left(s, s'\right) = \left\langle \boldsymbol{u}(s) \cdot \boldsymbol{u}\left(s'\right) \right\rangle = \exp\left(-\left|s - s'\right|/l_p\right), \tag{3}$$

We consider our linear chain taking into account interactions with other "links" (monomers) in the same chain and interactions with their environment. These interactions (bending energy) are described by an effective potential that represents the energy cost for their formation. The stability of the chain is determined by two forces, elastic with a negative sign, which leads the chain to a collapse, and another repulsive one with a positive sign, which causes the chain to be stretched. This energy cost is reflected in the chain in the form of free energy, for example, the number of conformations decrease with increasing end-to-end distance, but their free energy increases due to the high correlation that exists in the chain.

In continuous mechanic systems like a rod with stiffness constant k under the action of a force [12, 13], there is a correlated behavior in relation to its structure, described by the Eq. 3. Flexing generates a differentiable curve on the rod, where, at a point $r(s)$ of the curve there is a tangent vector $u(s)$ leading to a behavior similar to that described in Fig. 2b for linear chains. The Hamiltonian describing the internal energy of the rod of length i_c is given by Eq. 4, as follows:

$$\mathcal{H} = \frac{k}{2} \int_0^{l_c} \left(\frac{\partial \boldsymbol{u}(s)}{\partial s} \right)^2 ds. \tag{4}$$

Chains with high flexibility experience changes of direction at a distance of few "links" tending to turn to itself, while low flexibility chains tend to become rigid, because the two-segment correlation function in the chain decreases exponentially with the distance between them as shown in Eq. 3. By virtue of this, we propose a discretization of bending energy in order to be adapted to our chains, in this way, part of the internal energy of the chain which is described in terms of its configuration and which is equivalent to Eq. 4 is given by the following relation:

$$\mathcal{H} \cong H = \frac{k}{b} \sum_{i,j=1}^{N} \varepsilon_{ij} p_i, \tag{5}$$

where the weight function ε_{ij} can take values of (1) or (-1) depending on whether or not the direction of the *i-th* step changes as compared to the previous step (see Fig. 3) and p_i represents the probability that each step will find any of its accessible microstates, k is a constant of units of energy times distance and finally, our model adopts the $b = 1$ as the length of Kuhn.

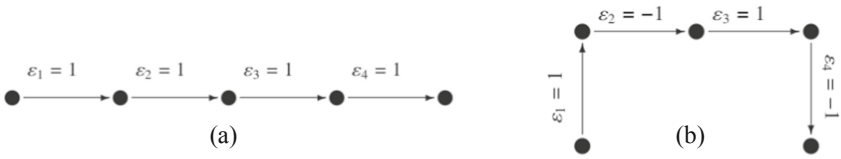

Fig. 3. 4-step 2d-chain that shows the value of the weight function ε_i used to compute the bending energy. Linear chain without deviation with its weight per step equal to 1, (a). Chain with mixed deviations, when direction changes ε_i adopts a weight equal to (-1), as is the case with steps 2 and 4, (b).

The bending energy, in its discrete version H, describes the behavior of the polymer chain from its tangential correlations, for example, for a highly correlated polymer chain (Fig. 3, a) this energy will be purely positive (high free energy) what is expected from the Hamiltonian described by the rod and the correlation given in Eq. 3.

The bending energy can be positive or negative depending on the winding of the chain. In our simulations the calculation of bending energy takes into account the term we call function weight as well as the relative probability of each step of the chain, which has the form of Eq. 6 [14].

$$p_i = \frac{e^{-gn_i}}{\sum_{j=1}^{3d} e^{-gn_i}} = \frac{1}{\sum_{j=1}^{3d} e^{-g(n_j - n_i)}}. \tag{6}$$

In Eq. 6, the sum runs through all possible $3d$ paths from the position occupied by the walker at each instant of time, including the address i, and g is a positive parameter which measures the intensity with which the walk avoids itself. For the sake of simplicity, in this work we implement the limiting case $g = \infty$, which corresponds in the $3d$ case to a discrete domain of probabilities $p_i(g = \infty) = [1/6, 1/5, 1/4, 1/3, 1/2, 1]$.

2.3 Anisotropy in Linear Chains

Inertia, Gyration Tensor and Asphericity. The main moments of the inertia tensor of the chains depend on their structure and they are correlated with their stability. The inertia tensor can be diagonalized, in function of their main moments, how we can see in the Eq. 7, as follows:

$$\hat{\boldsymbol{I}} = \begin{bmatrix} I_x & 0 & 0 \\ 0 & I_y & 0 \\ 0 & 0 & I_z \end{bmatrix}. \tag{7}$$

Each of the main moments of inertia (I_x, I_y, I_z) corresponds to a moment of inertia around one of the main axes, so a relationship between these moments allows us to carry out an analysis on the symmetry or asymmetry of each of the chains. In addition to the inertia tensor, the shape of the chains (like polymeric chains) can be characterized in gyration tensor terms [15, 16]. The gyration tensor is built from the dyadic of the position of the column vector $\boldsymbol{r_\alpha}$ in the center of mass of the system [17],

$$\boldsymbol{S} = \frac{1}{N}\sum_{\alpha}^{N} \boldsymbol{r_\alpha} \boldsymbol{r_\alpha^T} = \frac{1}{N}\begin{bmatrix} \sum_\alpha x_\alpha^2 & \sum_\alpha x_\alpha y_\alpha & \sum_\alpha x_\alpha z_\alpha \\ \sum_\alpha y_\alpha x_\alpha & \sum_\alpha y_\alpha^2 & \sum_\alpha y_\alpha z_\alpha \\ \sum_\alpha z_\alpha x_\alpha & \sum_\alpha z_\alpha y_\alpha & \sum_\alpha z_\alpha^2 \end{bmatrix}. \tag{8}$$

The inertia tensor $\boldsymbol{I}$ is directly related with the gyration tensor $\boldsymbol{S}$,

$$\boldsymbol{I} = \mathrm{Tr}(\boldsymbol{S})1 - \boldsymbol{S}, \tag{9}$$

were 1 is the unit tensor and $\mathrm{Tr}(\boldsymbol{S})$ is the gyration tensor trace. From the gyration tensor we can define the asphericity Δ [18] and the nature of asphericity Σ [19], represented by:

$$\Delta = \frac{3}{2}\frac{\mathrm{Tr}\left(\hat{\boldsymbol{S}}^2\right)}{\left(\mathrm{Tr}\left(\hat{\boldsymbol{S}}\right)\right)^2}, \Sigma = \frac{4\det\left(\hat{\boldsymbol{S}}\right)}{\left(\frac{2}{3}\mathrm{Tr}\left(\hat{\boldsymbol{S}}^2\right)\right)^{3/2}}, \tag{10}$$

$\hat{\boldsymbol{S}}$ is the following transformation:

$$\hat{\boldsymbol{S}} = \boldsymbol{S} - \frac{1}{3}\mathrm{Tr}(\boldsymbol{S})1. \tag{11}$$

For asphericity, we have $0 \leq \Delta \leq 1$, were $\Delta = 0$ correspond to an object completely symmetric and $\Delta = 1$, correspond to a completely stretched object, similar to a rigid bar. On the other hand, the nature of asphericity is limited by $-1 \leq \Sigma \leq 1$, were $\Sigma = -1$ represent a oblate object, like a disk, and $\Sigma = 1$, a prolate object [80, 97 Tese]. The combination of asperity and the nature of asphericity allows to identify the approximate shape of the configuration adopted by the three-dimensional chain. For comparative purposes, a transformation of these parameters can be adopted [19, 20] like:

$$\rho = 2\sqrt{\Delta} \in [0, 2], \theta = \frac{1}{3}\arccos(\Sigma) \in [0, \pi/3] \tag{12}$$

Using the parameters ρ and θ related to asphericity and the nature of asphericity we can have a different and more general perspective of the form adopted by the chains.

3 Results and Discussion

3.1 Energy of the Linear Chains

To study the energy of the random chains generated by our simulation, we analyzed the energy given by the interactions between "links" (monomers) in each chain, as well as the energy associated with the bending of the chains. As generated chains are homogeneous (identical links), like "homo-polymeric" chains, they are expected to show a uniform behavior or have a low amount of metastable states [6, 21].

In the contact potential described in Eq. 1, the value of the constant e_{ij} has the information about of interaction energy between the non-continuous and adjacent links. This constant adopts the value of -1, for each contact, thus generating a "folding" force in the chain, known in proteins as a hydrophobic force [7]. The sum of all the interactions in chain defines the energy of the system, called interaction energy E. To take into account the flexibility of the chain and, consequently, its tangent correlations, we proposed adding to the interaction term E, the bending energy H in its discrete version, proposed in Eq. 5.

In the Fig. 4 we can see the characteristic histograms of each energy for three-dimensional chains generated using our algorithm. The shape of the distribution is similar to the results obtained previously for the distribution of number of steps.

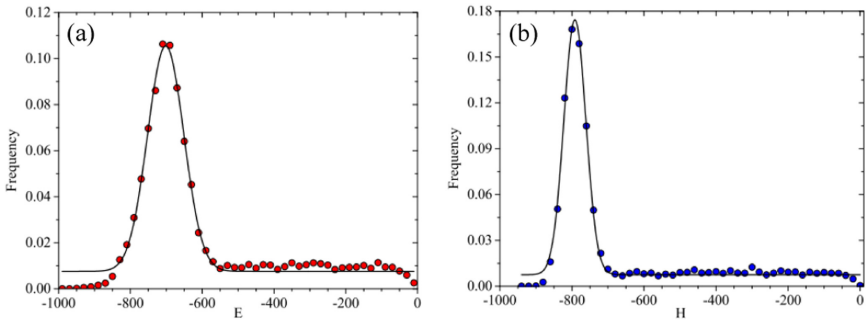

Fig. 4. Interaction energy E (a) and bending energy H (b) histograms, for three-dimensional chains. Gaussian distributions with standard deviations, $\sigma_E \cong 51$ and $\sigma_H \cong 31$, and mean values $\mu_E \cong -702$, and $\mu_H \cong -792$ respectively.

Even when considering both attractive and repulsive behavior of the chains, the resulting chains have negative energy, because in the SAW models for polymers in a good solvent, the attractions prevail over the repulsions [9, 10].

The total energy of the chain is described by the sum of interaction and bending energies, which determine the structural configuration. In Fig. 5a, the total energy distribution is shown. The most probable energy values are between -1650 and -1350 energy units, corresponding to long chains.

The mean values for the interaction energy and bending energy were computed for eleven thousand three-dimensional chains. Although was computed the mean values for the total (interaction plus bending) energy. All the energies were plotted as a function

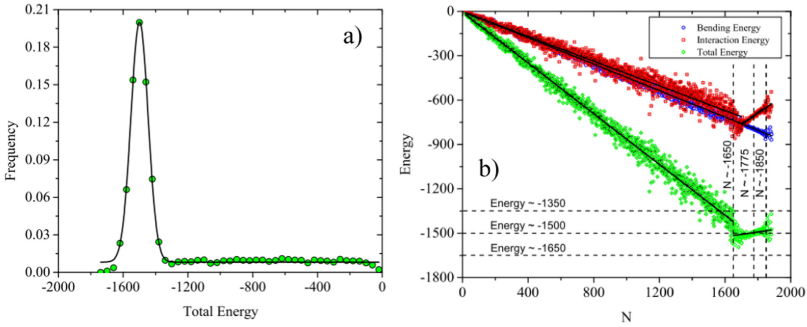

Fig. 5. Total Energy histogram $(E + H)$ for three-dimensional chains with mean with mean $\mu \cong -1499$ and standard deviation $\sigma \cong 53$ (a). Interaction energy E and bending energy H as a function of the number of steps N. The horizontal dotted lines represent the values between which the energies are distributed (see Fig. 4 and Fig. 5a). On the other hand, the vertical ones, represent the values between which distribute all sizes of the three-dimensional chains generated (b).

of N (Fig. 5b). The plots show a linear and uniform behavior for total energy (which is expected [6, 21]). However, when N is large ($\geq\sim$ 1650), the behavior of the interaction energy changes from decreasing to increasing, having less negative values, which can be interpreted as representative of more stretched chains, with fewer contacts but with small lengths of persistence still prevailing.

With the objective to better understand the behavior of energy, we have plotted the distribution of the size of chains. The great majority of the three-dimensional chains generated are large ($N > 1700$), how we can see in Fig. 6. These chains, with total energies between -1350 and -1650, belong to the second regime of the graph of the total energy and follow a Gaussian distribution (see Fig. 5). The rest of the chains, with

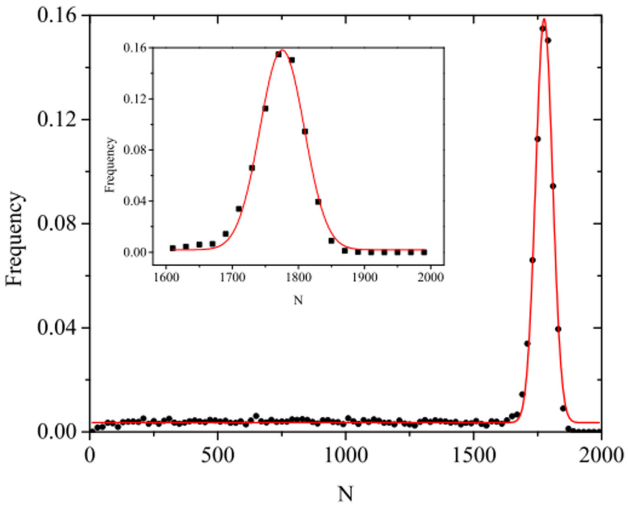

Fig. 6. Normalized histogram of the number of steps N *with* mean $\mu = 1775$ and standard deviation $\sigma = 33$. Behavior obtained for random chains in $3d$, ψ generated from $N' = 2400$ attempts. The inset illustrates the histogram in a wide interval in which a Gausian behavior occurs.

total energy between 0 and −1350, belong to the first regime of the energy graph and follow a uniform distribution.

In the "discrete" bending energy approach, the second regime does not appear (see Fig. 5b). This term has the same linear behavior, regardless of the presence of neighbours interacting with other links (monomers). The folding of the chains in the regime with large N adds negative energy to the system.

In the total energy graph of Fig. 5b, two regimes can also be seen due to the contribution of the interaction term. For chains of size below $N = 1775$ (mean value of N), the energy decreases with N at a rate of 0.86, practically twice the rate of decrease of each term separately, because the two energy contributes in this regime in the same proportion. For larger chains, the energy increases with N and the characteristic rate of this increase is 0.29. Here the different contributions of the two types of energy make the increase less significant than in the case of the interaction energy.

3.2 Inertia and Anisotropy

A typical linear chain with $N = 1772$ steps, generated by the simulation is shown in Fig. 8. This chain forms two clusters separated by a tail. The chain "escapes" from the first cluster and the interaction energy decreases because does not have neighbours that contribute to this energy. The flexibility of the chain is maintained causing the chain to continue folding even in the "bridge" that separates the clusters, and the bending energy remains constant (as we saw earlier). This represents a decrease in the interaction energy, restoring later, during the growth process, the original structure (Fig. 7).

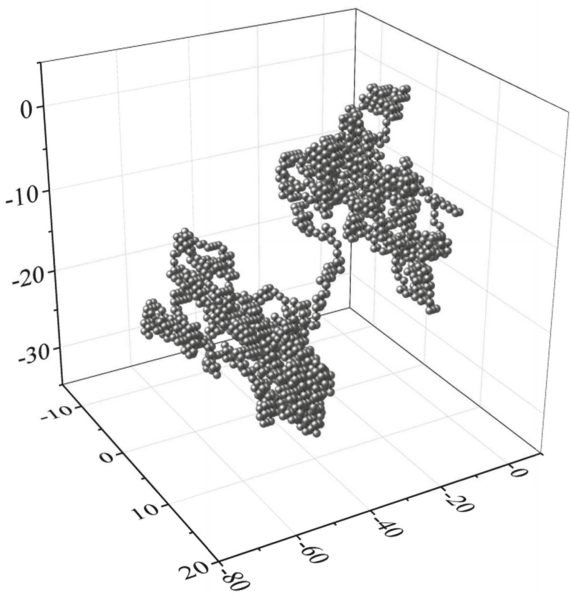

Fig. 7. Typical structure of $N = 1772$ generated by the simulation which shows the formation of two clusters. The spheres represent the links (monomers) of a linear (homo-polymeric) chain.

We plot three different views of main moments of inertia I_x, I_y and I_z and in each plane, a projection of them, see Fig. 8. It is observed that structurally the chains have a preference for adopting a stretched shape along the x axis. Chains like polymeric chains assume, preferably, an ellipsoidal or prolate shape [17, 22–24]. When analyzing our results, from the study of main moments of inertia, we can see that they correspond with this fact.

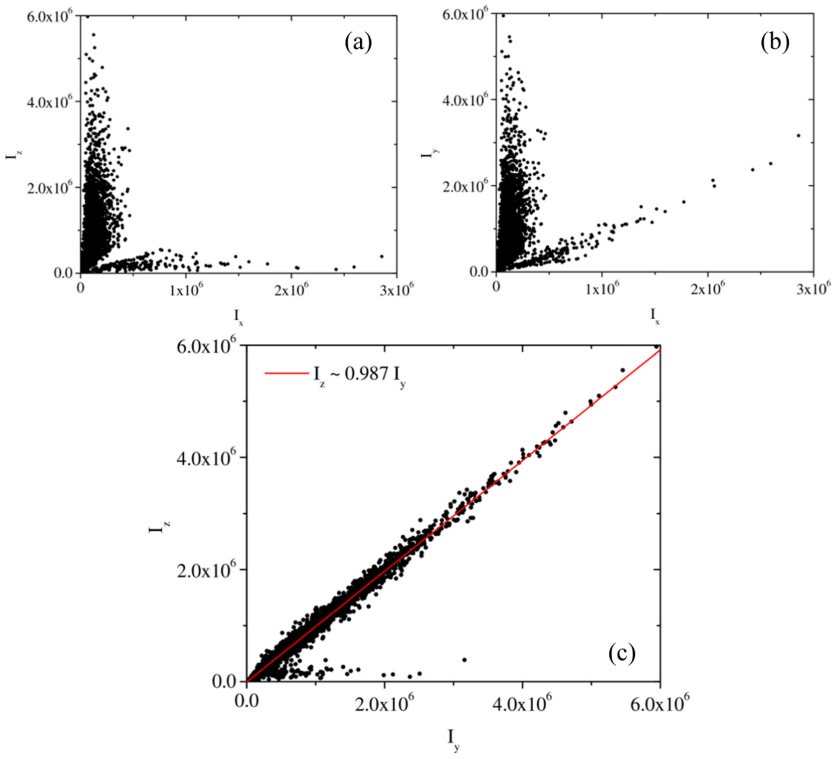

Fig. 8. Relationship between the main moments of inertia, (a): I_z vs. I_x; (b): I_y vs. I_x and (c): I_z vs. I_y. In (c), is illustrated how, structurally, the chains have a preference to adopt a "stretched" shape along the x-axis.

Figure 9 shows the distribution of asphericity values for the three-dimensional generated chains. It's possible to observe a maximum for the asphericity in $\Delta_{max} \approx 0.76$, in accordance with the values corresponding to these type of structures. On the other hand, we see that the occurrences in the case of the nature of asphericity are practically concentrated around the value $\Sigma = 1$, corroborating the same hypothesis. These distributions, as well as the behavior of the main moments of inertia, demonstrated that the three-dimensional chains generated prefer to adopt stretched structures, in general, like real polymeric chains.

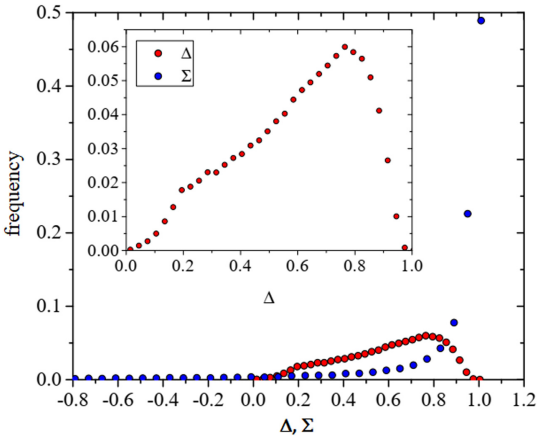

Fig. 9. Distributions of variables: asphericity (Δ), red dots, and nature of asphericity, blue dots, for three-dimensional random linear chains. The behavior of these distributions reveals a preferably prolate structure, from the position of the peaks of the frequencies. (Color figure online)

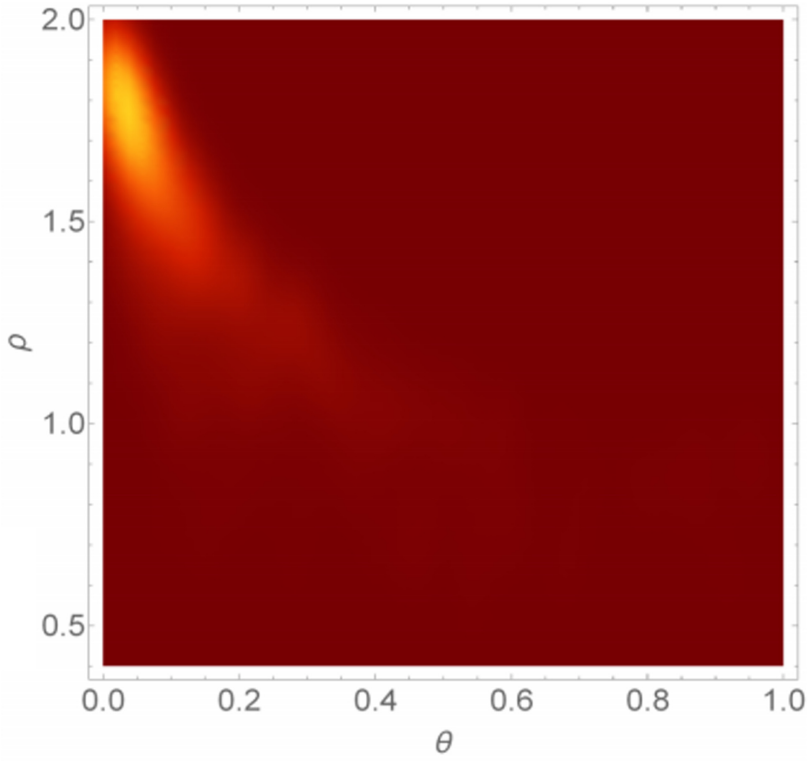

Fig. 10. Adopted configurations by linear chains. The yellow color represent high density of points, revealing a higher concentration of chains with high values of ρ and low values of θ. This graph shows the most likely prolate configuration that is generated by our model. (Color figure online)

In Fig. 10, we show a different perspective to analyze the form adopted by the three-dimensional linear chains generated. This graph shows a high density of point in the region corresponding to a low values of $\theta\left(\theta \approx \frac{\pi}{90}\right)$ and high values of $\rho(\rho \approx 1.78)$, which reflects in the understanding of the preferential behavior of our chains. The region of θ and ρ large is a forbidden region since the eigenvalues of tensor radius of gyration become negative, which is incompatible with real chains. The area below the yellow region (high densities), represents all configurations ranging from a totally prolific geometry at $\theta = 0$ like that of a rigid rod to a totally oblate structure of a rigid ring at $\theta = \frac{\pi}{3}$. From $\frac{\pi}{6}$, the form adopted by the chains is quite noticeable. For $\theta > \frac{\pi}{6}$ the shape is oblate and comparatively prolate for $\theta < \frac{\pi}{6}$. With respect to ρ, the lower this value, the structure becomes more and more spherical, resulting in a spherically symmetrical conformation for $(\pi/6; 0)$. Theoretically, for open polymers flexible, it is known that the adopted form is almost exclusively prolate and rarely spherical, which indicates a peak around $\theta = \frac{\pi}{40}$ and $\rho = 1.55$ [19].

4 Conclusions

Comparing the behavior of the E energy, which characterizes the monomer-monomer interactions of the chains, with the H energy, associated with its flexibility, we found that the chains start with clusters that increase in size, leading to an initial increase in their energy. When the chains reach a large number of steps, the interaction energy revealed that the chain stretches and escapes from the cluster, which results in a loss of interaction energy.

The behavior of the bending energy reveals that, in this escape regime, the chains keep the folding behavior they showed before the escape. This process lasts until the clusters reach a size comparable with the mean radius of gyration. The analysis presented in this work, including both the bending and interaction energies is important because it allows differentiating between chains of interaction energy but with different structures and hence different bending energies.

From analysis of inertia tensor and asphericity, we can conclude that the generated three-dimensional chains present anisotropy, with symmetry around one of the main axes of rotation. As a result, in general, our chains adopt a prolate structure, the same structure evident in real polymeric chains.

References

1. Flory, P.J.: Principles of Polymer Chemistry. Cornell University Press, Ithaca (1953)
2. Flory, P.J.: The configuration of real polymer chains. J. Chem. Phys. **17**(3), 303–310 (1949)
3. Madras, N., Sokal, A.: The pivot algorithm: a highly efficient Monte Carlo method for self-avoiding walk. J. Stat. Phys. **50**(1–2), 109–186 (1988)
4. Slade, G.: Self-avoiding walks. Math. Intell. **16**(1), 29–35 (1994). https://doi.org/10.1007/BF03026612
5. Figueirêdo, P.H., Moret, M.A., Coutinho, S., Nogueira, J.: The role of stochasticity on compactness of the native state of protein peptide backbone. J. Chem. Phys. **133**, 08512 (2010)

6. Boglia, R.A., Tiana, G., Provasi, D.: Simple models of the protein folding and of non-conventional drug design. J. Phys. Condens. Matter **16**(6), 111 (2004)
7. Tang, C.: Simple models of the protein folding problem. Phys. A Stat. Mech. Appl. **288**(1), 31–48 (2000)
8. Grosberg, A.Y., Khokhlov, A.R.: Statistical Physics of Macromolecules. AIP Press, New York (1994)
9. Rubinstein, M., Colby, R.H.: Polymer Physics. Oxford University Press, New York (2003)
10. Teraoka, I.: Polymer Solutions: An Introduction to Physical Properties. Wiley Inter-science, New York (2002)
11. Hsu, H.P., Paul, W., Binder, K.: Standard definitions of persistence length do not describe the local "intrinsic" stiffness of real polymers. Macromolecules **43**(6), 3094–3102 (2010)
12. Landau, L.D., Lifshitz, E.M.: Theory of Elasticity. Elsevier Sciences, New York (1986)
13. Schöbl, S., Sturm, S., Janke, W., Kroy, K.: Persistence-length renormalization of polymers in a crowded environment of hard disks. Phys. Rev. Lett. **113**(23), 238302 (2014)
14. Amit, D.J., Parisi, G., Paliti, L.: Asymptotic behavior of the "true" self-avoiding walk. Phys. Rev. B **27**(3), 1635–1645 (1983)
15. Solc, K.: Shape of random-flight chain. J. Chem. Phys. **55**(1), 335–344 (1971)
16. Rudnick, J., Gaspari, G.: The asphericity of random walks. J. Phys. A: Math. Gen. **30**(11), 3867–3882 (1997)
17. Hadizadeh, S., Linhananta, A., Plotkin, S.S.: Improved measures for the shape of a disordered polymer to test a mean-field theory of collapse. Macromolecules **44**(15), 6182–6197 (2011)
18. Aronovitz, J., Nelson, D.: Universal features of polymer shapes. J. Phys. **47**(9), 1445–1456 (1986)
19. Cannon, J.W., Aronovitz, J.A., Goldbart, P.: Equilibrium distribution of shapes for linear and star macromolecules. J. Phys. I Fr. **1**(5), 629–645 (1991)
20. Alim, K., Frey, E.: Shapes of semi-flexible polymer rings. Phys. Rev. Lett. **99**(19), 198102 (2007)
21. Dokholyan, N.V., Buldyrev, S.V., Stanley, H.E., Shakhnovich, E.I.: Discrete molecular dynamics studies of the folding of a protein-like model. Fold. Des. **3**(6), 577–587 (1998)
22. Theiler, J.: Estimating fractal dimension. J. Opt. Soc. Am. A, OSA **7**(6), 1055–1073 (1990)
23. Blavatska, V., Janke, W.: Shape anisotropy of polymers in disordered environment. J. Chem. Phys. **133**(18), 184903 (2010)
24. Rawdon, E.J., et al.: Effect of knotting on the shape of polymers. Macromolecules **41**(21), 8281–8287 (2008)